Fundamental J. Modern Physics, Vol. 3, Issue 2, 2012, Pages 125-155
Published online at http://www.frdint.com/

THEORY OF WELDING OF METALLIC PARTS IN MICROWAVE CAVITY APPLICATOR

SHANTANU DAS[1,*], AMIT BANSAL[2] and APURBA KUMAR SHARMA[2]

[1]Reactor Control Division
Bhabha Atomic Research Centre
Mumbai, India
e-mail: shantanu@barc.gov.in

[2]Department of Mechanical and Industrial Engineering
Indian Institute of Technology Roorkee
Roorkee, India

Abstract

We have been successfully welding bulk metals and dissimilar metals by microwave radiation, by using metal powder particles in the weld zone. In this paper, we have tried to explain the insight of electromagnetic field penetration into spherical conductive powder particles and its spatial oscillatory distribution. This new developed theoretical explanation here, gives insight as to how the entire weld zone volume becomes heat source; via absorption of microwave radiation, and thus this process of welding with microwave radiation, is with inertia less heat transfer, volumetric heating with inverted temperature profile.

1. Introduction

It is well known that the metals reflect microwave radiation, and have few microns of skin depth. Thus bulk metals cannot be heated as the AC Electromagnetic field penetrates 'skin-deep' that is about few micron at 2.45 GHz for copper, thus

Keywords and phrases: skin depth, spherical harmonics, scattering, refractive index, Effective Medium Approximation (EMA), Mie solutions, metal powder, resonance cavity, wave length.

*Corresponding author

Received September 21, 2012

most of the EM energy is reflected. But recently by use of the microwave radiation of 2.45 GHz, we have joined bulk metals of similar and dissimilar nature, (Copper, Mild Steel, Stainless Steel, Inconel), using metal powder of about 40 micron sizes. Refer Figure 1 for photographs of metals (bar-pipes) joined by microwave radiation [1-3]. Figure 2 gives scanning electron microscope observation showing regular cell like structure in the weld area and its uniformity. Our welding experiments are done in decimeter range of 2.45 GHz microwave radiation in resonating cavity of 900 Watt. As to how the metals in powder form absorb microwave radiation, the suitable theoretical explanation is still not made available. We have attempted to develop theoretical explanation of microwave energy absorption by metal particles of micron size, via Mie theory of electromagnetic scattering and diffraction [4-6]. The developed concept gives spherical harmonics in scattering of microwave radiation via spherical objects; and derives 'spatially' oscillatory transmission and reflection coefficients. These scattering coefficients require spherical Henkel's and spherical Bessel's function, and its approximate calculations are done via [10-21]. The profiles of Electromagnetic Energy absorbed inside the sphere are plotted and suitable explanation about its nature is derived. The basic penetration of EM field inside the conductive sphere of small size as explained in this paper, gives electromagnetic heating via loss tangent in Electric case and Joule (induction) heating in Magnetic case, is elaborated. This paper is not about advantages of microwave welding over conventional schemes; nor to discuss its metallurgical advantages of microstructures, mass transport, strength of joined metal parts, thermo-physics of microwave welding, thermal runaway; but to get into physics of absorption of electromagnetic energy, which is responsible for inertia less heat transfer, and inverted temperature profile and volumetric heating of join zones, while welding the bulk metal parts, via use of metal powders, in microwave resonance cavity applicator.

The paper is organized as seven main sections. Section 2 deals with basic microwave energy dissipation in material, concept of high loss case and low loss case, reflection of microwaves, concept of skin depth and effective conductivity, and reasons of high rate of microwave absorption at elevated temperatures in ionic and covalent type crystals. Section 3 gives idea about interaction of electromagnetic radiation with spherical objects scattering, the idea of refraction in highly conductive interface, Effective Media Approximation (EMA) for metal conductor sphere coated with thin mantle of insulator, expansion of plane waves into spherical harmonics, partial electric and magnetic modes and mode functions on a sphere, spatially oscillating reflection and transmission coefficients via Mie solution. Section 4 gives

elaboration on the power per unit volume absorbed scattered and terminated, and approximations for Mie coefficients of transmission and reflections. Section 5 deals with expansion coefficients of Mie solution with plots of power inside the spherical sample and field plots, for various cases of dielectric permittivity and metal powder radius, its coating thickness. Section 6 is observation about several plots and discussions derivations of the paper to arrive at probable theory of heating via microwave radiation as done in experiments of metal welding, giving elaboration on physical construction of microwave radiation penetration its electric heating its magnetic heating and thereby inverted heat profile in heat conduction diffusion equation. This section is followed by conclusions and references.

2. Microwave Energy Dissipation in Material

Any of the heating process that uses electromagnetic energy can be characterized by skin depth and reflection coefficient; which are function of material properties mainly dielectric permittivity and effective conductivity. Absorption of microwave radiation depends upon material properties characterized via imaginary dielectric permittivity ε'' (where $\varepsilon = \varepsilon' - i\varepsilon''$) loss tangent that is $\tan\delta = \varepsilon''/\varepsilon'$, or effective conductivity $\sigma_{\text{eff}} \sim \omega\varepsilon''$. Materials are characterized by high loss for $\tan\delta \geq 10^{-1}$, and low loss for $\tan\delta \leq 10^{-3}$. At normal room temperature, dielectric losses of low-absorption materials are caused by displacement of bound charge carriers in such a process as atomic lattice vibrations and dipole reorientation. Among the low loss materials are for example pure-oxides (Al_2O_3, BeO, SiO_2) and nitrides (AlN, BN, Si_3N). At the elevated temperatures microwave absorption in most material grows sharply. This is due to onset of another process. This is characteristic of both with ionic (Al_2O_3, ZnO_2) and covalent (Si_3N, AlN) bonding. A sharp increase in microwave loss factor starts at about $0.4 - 0.5T_m$, T_m, the melting temperature of the material; as the bonding between ions in ionic crystal, and covalent bonds, starts breaking and electrons in these materials begin to populate at conduction band. Thus as the temperature rises more and more microwave radiation gets absorbed and this is cause of thermal runaway and quick melting of materials under microwave radiation.

The frequency dependence of dielectric permittivity determines the peculiar feature of heating by EM radiation of different frequency. In conventional furnace

heating, energy is transferred to the material by thermal electromagnetic radiation with maximum intensity in infrared (IR) range. The skin depth (penetration) of IR $\omega \geq 10^{13}\mathrm{s}^{-1}$ is very small $l \leq 10^{-4}\mathrm{m}$ in most solids. Therefore the energy absorption is localized within thin layers near the surface. As a result the conventional heating essentially depends on heat transfer from hotter-near surface region to colder bulk of material. In microwave frequency range, the absorption properties of non-metallic material vary greatly, the loss factor $\tan\delta$ varies at room temperature from 10^{-4} - 10^{-3} (pure alumina silicon nitride) up to 1 and higher (in carbides, borides, some oxides, inter-metallic compounds). Correspondingly, the penetration depth varies from meters to fraction of a millimeter. Thus the dielectric properties of material along with temperature chemical composition microstructure are of paramount importance for efficient use of microwave radiation for material processing.

In a DC electric field the local density of the energy released at any point of the material is $w(\mathbf{r}) = \sigma|\mathbf{E}(\mathbf{r})|^2$ in $\mathrm{Watt/cm}^3$, σ denoting the static conductivity of material. For an AC field, we can write from dielectric loss (the imaginary part of the dielectric complex function; $\varepsilon = \varepsilon' - i\varepsilon''$) an effective conductivity as $\sigma_{\mathrm{eff}} = \varepsilon_0\varepsilon''\omega$; ($\varepsilon_0 = 8.8\times10^{-12}$ F/m) which manifests as factor for dielectric heating in microwave radiation. Similarly, magnetic losses $(\mu = \mu' - i\mu'')$ can manifest as effective conductivity in AC field as $\sigma_{\mathrm{eff}} = \mu_0\mu''\omega$, ($\mu_0 = 4\pi\times10^{-7}$ H/m). So in general, we may write total energy density (Watt/Volume) released in AC field as follows

$$w(\mathbf{r}) = \omega(\varepsilon_0\varepsilon''|\mathbf{E}(\mathbf{r})|^2 + \mu_0\mu''|\mathbf{H}(\mathbf{r})|^2)/2. \quad (1)$$

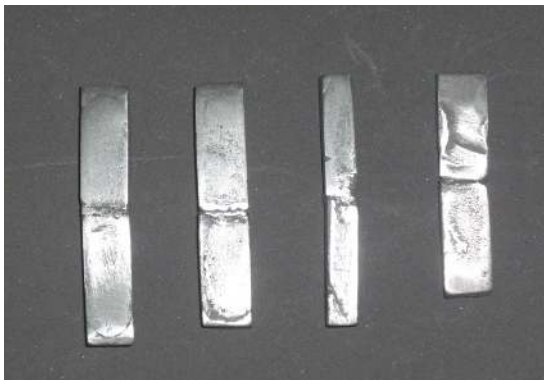

(1a) SS-316 bar

(1b) Steel pipe

Figure 1. Photographs of metal joints via microwave radiation.

In a Microwave oven with 2.45 GHz, the standing wave patterns for electric and magnetic field maxima $E_{\max}$ and $H_{\max}$ are separated by about 3 cm, that is, $\lambda/4$ of microwave signal of wavelength 12.2 cm, in free space. This separation is for single mode cavity; though presence of mode stirrer makes the fields uniform. One can therefore place the sample at $E_{\max}$ position or $H_{\max}$ position, for electric heating or magnetic heating by comparing the values of $\varepsilon_0\varepsilon'' E_{\max}^2$ and $\mu_0\mu'' H_{\max}^2$. Thus loss factor of permittivity $(\varepsilon = \varepsilon' - i\varepsilon''$, or $\tan\delta_e = \varepsilon''/\varepsilon')$ and permeability $(\mu = \mu' - i\mu''$, or $\tan\delta_m = \mu''/\mu')$ are primarily responsible for absorption of microwave energy, of electric type and magnetic type.

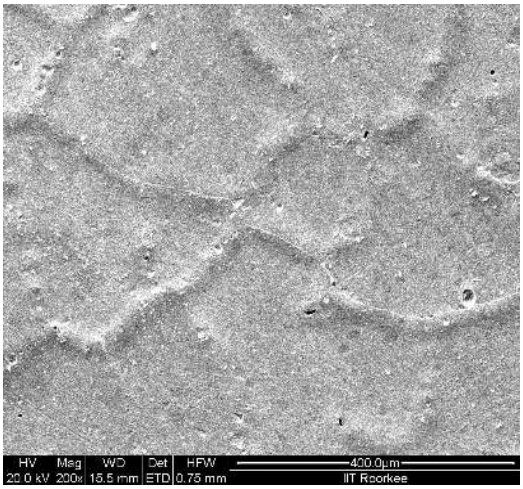

Figure 2. Scanning electron microscope observation.

Depth of penetration of AC EM field in dielectric with loss tangent [4] is given as

$$l = \frac{c}{\omega}\sqrt{\frac{2\left[1+\sqrt{1+(\tan\delta)^2}\right]}{\varepsilon'(\tan\delta)^2}} \cong \frac{c}{\omega}\sqrt{\frac{2}{\varepsilon''}}. \tag{2}$$

Here $c = 3\times10^{10}$ cm/s, and $\omega = 2\pi f$. At 2.45 GHz, for relative permittivity of $\varepsilon = 3 - i0.003$, $\varepsilon = 3 - i1$ and $\varepsilon = 3 - i300$; the penetration depths are 1566 cm, 6.8 cm and 0.156 cm, respectively, with loss tangent as 0.00099, 0.333 and 100. For a normal incident of microwave on a plane boundary between the material and vacuum, the fraction of reflected power [4] is

$$\mathbf{R} = \frac{1-\sqrt{2\varepsilon'\left[1+(\tan\delta)^2\right]}+\varepsilon'\sqrt{1+(\tan\delta)^2}}{1+\sqrt{2\varepsilon'\left[1+(\tan\delta)^2\right]}+\varepsilon'\sqrt{1+(\tan\delta)^2}}. \tag{3}$$

For the case of highly absorptive materials, classified as $\tan\delta \geq 0.1$, the effective conductivity is typically so large that a strong reflection of radiation from surface inhibits 'bulk' microwave heating. The absorbed fraction of microwave power can be estimated approximately as [4]:

$$1 - \mathbf{R} \cong 2\sqrt{\frac{2}{\varepsilon'\tan\delta}}. \tag{4}$$

Bulk metal cannot be heated in microwave radiation. The AC EM field penetrates

skin deep, thus most of the microwave energy is reflected. For copper with conductivity $\sigma = 5.8 \times 10^7$ S/m at 2.45 GHz, with free space permeability $\mu_0 = 1.2566 \times 10^{-6}$ H/m, the skin depth $l = 1\sqrt{\pi f \sigma \mu_0}$ is 1.3 micron. Iron having static conductivity about four-five times less will therefore have skin depth of about 2.5-3 microns. At this microwave frequency 2.45 GHz, the Magnesium, Tungsten and Zinc metal have skin depth as 2.17 micron, 2.3 micron and 2.54 micron, respectively. Therefore metal-particle of size comparable to the skin depth, can couple microwave radiation. Indeed compacted powder of metal can couple to microwave, with particle size of few microns. From the above discussions, we write the expression that gives microwave energy dissipation as [4, 6]

$$w(\mathbf{r}) = \frac{1}{2}\left[\omega\varepsilon''|\mathbf{E}(\mathbf{r})|^2 + \omega\mu''|\mathbf{H}(\mathbf{r})|^2 + \sigma_c|\mathbf{E}(\mathbf{r})|^2 + \sigma_i|\mathbf{E}(\mathbf{r})|^2\right] \tag{5}$$

with σ_c electronic conductivity, σ_i ionic conductivity. The above has components as first one, dielectric loss, owing to re-orientation or distribution of induced or permanent dipoles. The second one is the magnetic loss owing to re-orientation of magnetic domains. The third one is Joule loss due to currents with electrons and ions as charge carriers. The Watt/Volume, of above expression (5), requires knowledge of the local amplitudes and distribution of EM fields inside the particle, which is derived from full solution of Maxwell's equation. For example, a highly conductive sample $\sigma = 5.8 \times 10^7$ S/m will be having effective dielectric $\varepsilon = i(\sigma / \omega\varepsilon_0)$, that is about $i(4 \times 10^8)$ at 2.45 GHz, a very large $\tan\delta$, will absorb EM energy.

Assume a spherical particle with $\mu'' = 0$ and with low dielectric loss tangent $\varepsilon'' << 1$, in uniform electric field E_0. The quasi static case [4] is assumed with $|\varepsilon kR| << 1$, where R is the radius of sphere, k is free space wave number (that is, ω/c), gives $E_{\text{inside}} = 3E_0/(\varepsilon + 2)$, the field inside sphere. The field inside is attenuated if $\varepsilon > 1$, the actual case. The Electric-energy absorbed (call electric heating) by this sphere is [4]

$$W_E = \frac{1}{2}\omega\left(\frac{3E_0}{\varepsilon + 2}\right)^2 \varepsilon_0\varepsilon''\left(\frac{4}{3}\pi R^3\right) = 6\pi\varepsilon_0\varepsilon'' R^3\omega E_0^2 / |\varepsilon + 2|^2. \tag{6}$$

Similarly we write Magnetic-energy absorbed (call magnetic heating) by magnetic losses in sphere kept in uniform magnetic field H_0 as [4]

$$W_M = 6\pi\mu_0\mu'' R^3 \omega H_0^2 / |\mu + 2|^2. \quad (7)$$

For conductive material, the external electric field may be suppressed to a large extent inside the metallic sphere, even when the radius is small compared to skin depth. Then, we may assume that heating cannot be due to electric field absorption. We may now say then heating of such a particle be more efficient if kept in magnetic field maxima $H_{\max}$. Though the efficient energy absorbed is magnetic in nature, for this highly conductive particle, yet heating is electric type, Joule heating. The magnetic field which has penetrated inside the particle, 'induces' currents in the sample and this current is responsible for heating the particle. But a point is mentioned that while particle size is smaller than the skin depth, the heating (electric/magnetic) is volumetric in nature, as given by above formulas (6) and (7).

Usually the material that has significant magnetic losses $\sim \omega\mu'' H^2$, also exhibits 'strong dispersion' of μ and it can be assumed that in microwave ranges of ω, the relative permeability $\mu \sim 1$ for most materials. Thus optimum heating of small samples with high conductive samples with low dielectric loss $\varepsilon'' << 1$ occurs in $E_{\max}$ of standing wave applicator (oven).

3. Microwave Interaction with Spherical Metal Particles with Dielectric Oxide Mantle - The Principle of Scattering

3.1. General interaction of microwave with conductive material

A very simple and naive way to visualize the electromagnetic wave interaction with metal is via Snell's law of refraction that is relative refractive index is $m = \sin\theta_i / \sin\theta_r$. Whereas the metals exhibit a very high value of refractive index, indicate that for any incident angle the refraction angle θ_r tends to zero, meaning that any incident electromagnetic radiation falling on the plane metal surface, will bend towards the normal, irrespective of incident angle, [6], Figure 10a. The propagation of the refracted electromagnetic radiation, inside highly conductive material is always perpendicular to the surface of boundary, irrespective of the incident angle. But till what point inside the metal does the radiation propagate, obviously up to the skin depth (that is about few microns in pure metals); and most of the energy of radiation is reflected back from the plane metal boundary. This interaction is a surface phenomenon [6]. That is, while EM radiation is incident on

the metal sheet; it induces collective oscillations of 'surface conduction electrons'. The real wave propagation will occur at the surface (*xy* directions) only at resonance condition, and decaying evanescently in the *z*-direction, up to skin depth. The resonance condition, will have no reflection though, happens at negative value of real part of dielectric permittivity of metals at particular frequency. This surface (resonance) phenomenon is shown in Figure 6b. Reflection from metal sheet is though almost 100% (except for surface resonance) but this is not true for metal sphere having radius of curvature less than the wavelength of radiation inside the metals. The order of wavelength of radiation inside the metal is $\lambda_{inside} \sim 2\pi l$, that is in the order of skin depth. A radiation of frequency 2.45 GHz in the free space having wave length of 12.2 cm will have about 10 microns of wavelength inside small copper sphere. Therefore for small metal spheres of radius of few tens of microns there is possibility of penetration of radiation into the sphere, and by virtue of Snell's law the entire radiation is refracted normal to sphere surface concentrating towards the centre of sphere, Figure 10b. This surface phenomena get bounded when the metal particles small with circumference are comparable to wavelength inside metal, that is, $2\pi R \sim \lambda_{\text{inside}}$. This interaction is depicted in Figure 6b.

A plane wave of electromagnetic is diffracted by an object placed in its path. The various interactions are summarized in Figure 3, where a spherical object is placed in an electromagnetic field having incident wavelength of the radiation as λ. We are interested in the elastic scattering, of electromagnetic radiation and spherical object. The nature of scattering, depends on wavelength of incident radiation, that is, λ; the size parameter $x = 2\pi R / \lambda = kR$; where R is the radius of spherical particle, k is the free space wave number $(k = 2\pi / \lambda)$; and complex refractive index, $m = \text{Re}(m) - i\,\text{Im}(m)$ of the particle with respect to the surrounding. Elastic scattering is classified as Rayleigh's scattering; characterized by non-absorbing spherical particles of small spheres $(|x| << 1$, more specifically $|mx| << 1)$ and Mie scattering where object is still spherical, yet no size restrictions and assumes absorbing/non-absorbing particles [6]. We shall be taking Mie scattering and develop the theory of microwave absorption and its heating of small micron sized metal particles; used for welding of bulk metals, in microwave oven. Let us take microwave radiation of 2.45 GHz; having the wave length in free space 12.2 cm, in free space. The spherical particles what we are using as powder of metals (copper, nickel, iron, silver, etc.) for welding are having size $R = 20\,\mu\text{m}$. Thus the size factor x in our case is 1.03×10^{-3}, thus $x << 1$.

The core of metal particle actually is surrounded by 'oxide' layer a dielectric. This 'oxide-layer' prevents the percolation of conductivity between the particles, and increases the dielectric heating. The thickness of this mantle of dielectric oxide on the conductive powder is about 0.3 to 0.6 microns.

Effective Medium Approximation [9, 23] (EMA) gives resultant dielectric permittivity for a spherical core with parameter ε_c surrounded by insulator oxide ε_i of relative thickness $d = t/R$, where t is the thickness of oxide-mantle, and R is the radius of core; via following quadratic equation, for relative volumetric concentration of the core solid C, [9].

$$4\beta\varepsilon_{\text{eff}}^2 + 2[\beta(3C-2) + \varepsilon_i(\gamma - 3\alpha C)]\varepsilon_{\text{eff}} + \varepsilon_i[\gamma(3C-2) - 2\alpha C] = 0. \qquad (8)$$

The parameters are

$$\xi = 1 + d,\ \gamma = 2\varepsilon_i + \varepsilon_c + [2(\varepsilon_c - \varepsilon_i)/\xi^3],\ \beta = 2\varepsilon_i + \varepsilon_c + [(\varepsilon_i - \varepsilon_c)/\xi^3],$$

and

$$\alpha = [1 - (1/\xi^3)][2\varepsilon_i + \varepsilon_c - \{6/((1-\xi^3)(\varepsilon_c - \varepsilon_i)(\ln\xi))\}] + [3\varepsilon_c/\xi^3].$$

For instant placing $\varepsilon_i = 4$, $\operatorname{Re}\varepsilon_c = 12$, $d = 0.01$, we get $\gamma = 35.53$, $\beta = 4.47$, $\alpha = 108$; and for $C = 0.6$, the effective permittivity is obtained from the quadratic equation of EMA as $\operatorname{Re}\varepsilon_{\text{eff}} = 71$.

For $\operatorname{Im}\varepsilon_c = 10^4$, we get $\gamma = 2.94 \times 10^4$, $\beta = 0.03 \times 10^4$, $\alpha = 2.94 \times 10^4$ and for $C = 0.6$, the effective permittivity from quadratic equation of EMA as $\operatorname{Im}\varepsilon_{\text{eff}} = 3.23$.

Therefore a core of highly conductive sphere of $\varepsilon_c = 12 + i10^4$ with an insulating mantle of $\varepsilon_i = 4 - i0$, of mantle thickness on the core of $d = t/R$, is making the effective permittivity as $\varepsilon_{\text{eff}} = 12 - i3.23$. Physically we may interpret these phenomena as; the presence of a thin mantle is helping the electromagnetic radiation to penetrate the sphere to a greater depth towards the centre of sphere, else the penetration of radiation would have been limited to skin deep that is only at surface. Figures 7-8 elaborate this with Figure 9. This observation makes us believe that presence of thin insulating mantle helps the electromagnetic radiation to penetrate into the volume, thereby enhancing volumetric heating; else it would have

been surface heating for pure conductive core sphere. This phenomenon is explained via Mie solution in subsequent sections and in Figures 9 and 7.

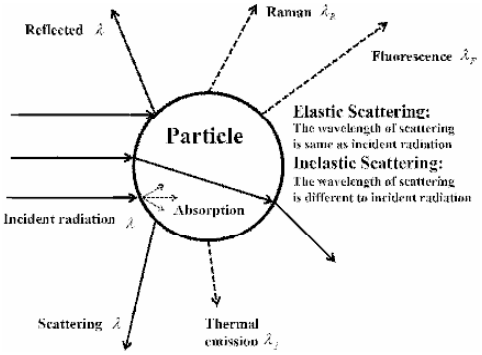

Figure 3. Various modes of scattering of electromagnetic radiation by spherical particle.

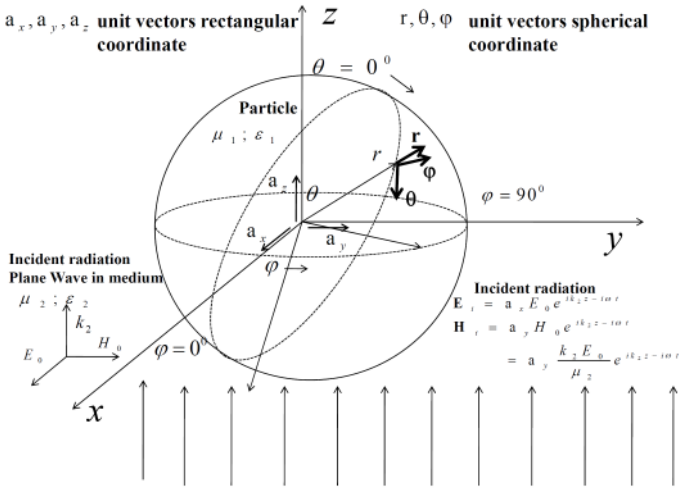

Figure 4. Plane wave, travelling in z direction (in medium 2), strikes a sphere (medium 1); the rectangular and spherical coordinates are marked.

3.2. Expansion of plane incident microwave field in spherical harmonics

A periodic electromagnetic (EM) wave, incident on a material body of any description (in our case spherical), gives rise to a forced oscillations of ‘free’ as well as ‘bound’ charges, in phase or in synchronism with the applied field. This constrained movement of free or bound charges set up in turn a ‘secondary’ field both inside and outside the body (particle). We assume the particle (body)

dimensions are larger than the relaxation lengths of the free and bound charges. The resultant field at any point is then 'vector' sum of primary and secondary fields [4, 6]. In general the forced oscillations fail to match the conditions prevailing at the instant the primary field was first established. To ensure fulfillment of the boundary conditions at all times a transient term must be added from the natural modes with suitable amplitudes [6]. Such transient oscillations, however, are quickly damped by absorption and radiation losses, leading only steady state, and those are synchronous terms. We are interested in the steady state terms, which ultimately decide the particle's way of absorption of the incident microwave radiation.

Refer Figure 4, the Electric and Magnetic fields as marked for plane (incident) wave in medium 2 travelling in z direction, are represented (expanded) in spherical harmonics as [4-6]:

$$\mathbf{E}_i = \mathbf{a}_x E_0 e^{ik_2 z - i\omega t} = E_0 e^{-i\omega t} \sum_{n=1}^{\infty} i^n \frac{(2n+1)}{n(n+1)} (\mathbf{m}^{(1)}_{o,1,n} - i\mathbf{n}^{(1)}_{e,1,n}), \tag{9}$$

$$\mathbf{H}_i = \mathbf{a}_y H_0 e^{ik_2 z - i\omega t} = -\frac{k_2 E_0}{\mu_2 \omega} e^{-i\omega t} \sum_{n=1}^{\infty} i^n \frac{(2n+1)}{n(n+1)} (\mathbf{m}^{(1)}_{e,1,n} + i\mathbf{n}^{(1)}_{o,1,n}), \tag{10}$$

$$\mathbf{m}^{(1)}_{\substack{o \\ e},1,n} = \pm \frac{1}{\sin\theta} j_n(k_2 R) P_n^1(\cos\theta)^{\cos}_{\sin} \varphi.(\boldsymbol{\theta}) - j_n(k_2 R) \frac{\partial P_n^1}{\partial \theta}^{\sin}_{\cos} \varphi.(\boldsymbol{\varphi}), \tag{11}$$

$$\mathbf{n}^{(1)}_{\substack{o \\ e},1,n} = \frac{n(n+1)}{k_2 R} j_n(k_2 R) P_n^1(\cos\theta)^{\sin}_{\cos} \varphi.(\mathbf{r}) + \frac{1}{k_2 R} [k_2 R j_n(k_2 R)]' \frac{\partial P_n^1}{\partial \theta}^{\sin}_{\cos} \varphi.(\boldsymbol{\theta})$$

$$= \pm \frac{1}{k_2 R \sin\theta} [k_2 R j_n(k_2 R)]' P_n^1(\cos\theta)^{\cos}_{\sin} \varphi.(\boldsymbol{\varphi}). \tag{12}$$

The prime denotes differentiation with respect to argument $k_2 R$. The spherical Bessel's functions of size parameter [6] $x = k_2 R$ are represented as $j_n(x)$, and Legendre polynomials of first kind are $P_n^1(\cdot)$. The above expression (9-12) is EM plane wave expansion in spherical harmonics. R is radius of sphere particle on which the plane wave is incident, the sphere is at the origin. The EM properties of sphere particle are represented as ε_1, μ_1 while the surrounding has EM properties represented as ε_2, μ_2. Therefore the refractive index of the spherical particle

compared with surrounding is $m = \sqrt{(\varepsilon_1\mu_1)/(\varepsilon_2\mu_2)}$; actually a complex quantity, [4, 6].

3.3. Reflection and transmission of EM field inside and outside spherical particle

The plane wave now gets reflected from the particle, and for $r > R$, the reflected EM components are

$$\mathbf{E}_r = E_0 e^{-i\omega t} \sum_{n=1}^{\infty} i^n \frac{2n+1}{n(n+1)} (a_n^r \mathbf{m}_{o,1,n}^{(3)} - ib_n^r \mathbf{n}_{e,1,n}^{(3)}), \tag{13}$$

$$\mathbf{H}_r = -\frac{k_2}{\omega\mu_2} E_0 e^{-i\omega t} \sum_{n=1}^{\infty} i^n \frac{2n+1}{n(n+1)} (b_n^r \mathbf{m}_{e,1,n}^{(3)} + ia_n^r \mathbf{n}_{o,1,n}^{(3)}). \tag{14}$$

The transmitted component expressions for EM fields, when $r < R$, are

$$\mathbf{E}_t = E_0 e^{-i\omega t} \sum_{n=1}^{\infty} i^n \frac{(2n+1)}{n(n+1)} (a_n^t \mathbf{m}_{o,1,n}^{(1)} - ib_n^t \mathbf{n}_{e,1,n}^{(1)}), \tag{15}$$

$$\mathbf{H}_t = -\frac{k_1}{\omega\mu_1} E_0 e^{-i\omega t} \sum_{n=1}^{\infty} i^n \frac{(2n+1)}{n(n+1)} (b_n^t \mathbf{m}_{e,1,n}^{(1)} + ia_n^t \mathbf{n}_{o,1,n}^{(1)}). \tag{16}$$

The functions $\mathbf{m}_{e}^{(3)}_{o,1,n}$ and $\mathbf{n}_{e}^{(3)}_{o,1,n}$ comes when $j_n(x)$ appearing in plane wave expansions is replaced by spherical Henkel's functions $h_n^{(1)}(x)$. Also note that k_1 replaces k_2, inside the sphere particle that is in the transmitted expression, to get the EM fields inside the particle. For the boundary at $r = R$, we have properties, $k_1 = mk_2$, $x = k_2 R$, $k_1 R = mx$ and $m = \sqrt{(\varepsilon_1\mu_1)/(\varepsilon_2\mu_2)}$. Say for metal particles if the refractive index is very large, the wavelength of the EM transmitted into the metal is very small, that is of the order of skin depth.

The boundary conditions [4] at $r = R$ are

$$(\mathbf{r}) \times (\mathbf{E}_i + \mathbf{E}_r) = (\mathbf{r}) \times \mathbf{E}_t, \tag{17}$$

$$(\mathbf{r}) \times (\mathbf{H}_i + \mathbf{H}_r) = (\mathbf{r}) \times (\mathbf{H}_t). \tag{18}$$

From above we get two pair of inhomogeneous equations for the expansion

coefficients

$$a_n^t j_n(mx) - a_n^r h_n^{(1)}(x) = j_n(x), \tag{19}$$

$$\mu_2 a_n^t [mxj_n(mx)]' - \mu_1 a_n^r [xh_n^{(1)}(x)]' = \mu_1 [xj_n(x)]' \tag{20}$$

and

$$\mu_2 m b_n^t j_n(mx) - \mu_1 b_n^r h_n^{(1)}(x) = \mu_1 j_n(x), \tag{21}$$

$$b_n^t [mxj_n(mx)]' - mb_n^r [xh_n^{(1)}(x)]' = m[xj_n(x)]'. \tag{22}$$

From above we get the magnetic and electric reflection coefficients as

$$a_n^r = -\frac{\mu_1 j_n(mx)[xj_n(x)]' - \mu_2 j_n(x)[mxj_n(mx)]'}{\mu_1 j_n(mx)[xh_n^{(1)}(x)]' - \mu_2 h_n^{(1)}(x)[mxj_n(mx)]'}, \tag{23}$$

$$b_n^r = -\frac{\mu_1 j_n(x)[mxj_n(mx)]' - \mu_2 m^2 j_n(mx)[xj_n(x)]'}{\mu_1 h_n^{(1)}(x)[mxj_n(mx)]' - \mu_2 m^2 j_n(mx)[xh_n^{(1)}(x)]'}$$

$$= -\frac{\varepsilon_1 j_n(mx)[xj_n(x)]' - \varepsilon_2 j_n(x)[mxj_n(x)]'}{\varepsilon_1 j_n(mx)[xh_n^{(1)}(x)]' - \varepsilon_2 h_n^{(1)}(x)[mxj_n(mx)]'}. \tag{24}$$

This gives the transmitted coefficients inside sphere particle as follows

$$a_n^t = \frac{j_n(x) + a_n^r h_n^{(1)}(x)}{j_n(mx)},$$

$$b_n^t = \frac{m[xj_n(x)]' + mb_n^r (xh_n^{(1)}(x)]'}{[mxj_n(mx)]'} = \frac{j_n(x) + b_n^r h_n^{(1)}(x)}{mj_n(mx)}. \tag{25}$$

For particles having very large conductivity or inductive capacity $(\varepsilon_1 / \varepsilon_2)$ relative to surroundings, and radius (R) of sphere particles not too small size (say, comparable to wavelength of EM radiation in medium-1 sphere); the above coefficients of reflection can be simplified by taking following asymptotic approximations [7]

$$j_n(mx) \cong \frac{1}{mx} \cos\left(mx - \frac{n+1}{2}\pi\right), \tag{26}$$

$$[mxj_n(mx)]' \cong \sin\left(mx - \frac{n+1}{2}\pi\right), \tag{27}$$

$$h_n^{(1)}(mx) \cong \frac{1}{mx}(-i)^{n+1}e^{imx}. \tag{28}$$

With these we get

$$a_n^r \cong -\frac{j_n(x)}{h_n^{(1)}(x)}, \qquad b_n^r \cong -\frac{[xj_n(x)]'}{[xh_n^{(1)}(x)]}. \tag{29}$$

Since $h_n^{(1)}(x) = j_n(x) + in_n(x)$, these coefficients above can be put in form

$$a_n^r \cong ie^{i\gamma_n}\sin\gamma_n, \qquad b_n^r \cong ie^{i\gamma_n'}\sin\gamma_n', \tag{30}$$

where $\tan\gamma_n = \frac{j_n(x)}{n_n(x)}$ and $\tan\gamma_n' = \frac{[xj_n(x)]'}{[xn_n(x)]'}$.

These are Mie solution of the Maxwell equation, which does not distinguish between different types of losses (electric/magnetic/Joule). They combine dielectric and Joule losses in a single dielectric function, that is,

$$\varepsilon_1 = \varepsilon + i\frac{\sigma_e + \sigma_i}{\omega} = \varepsilon' - i\varepsilon'' + i\frac{\sigma_e + \sigma_c}{\omega} \tag{31}$$

and considers them as unified dielectric, where ε is used in microwave energy absorption formula (5). Moreover, a_n^r and b_n^r are explicitly depending on the refractive index $m = \sqrt{\varepsilon_1\mu_1}$ (assuming the medium surrounding the sphere particle is free space $\mu_0 = \varepsilon_0 = 1$), indicates complete separation of dielectric and magnetic losses is difficult, in general. Calculations of these Mie coefficients are described in details via various methods in [10-21].

3.4. Physical interpretations of mode functions

When metallic spherical particles are irradiated, oscillating electric field causes collective oscillations of conduction electrons in metals. The Columbic attraction between the negative and positive charged nuclei (and repulsion among electrons) causes a restoring force to arise when electron cloud is displaced relative to nuclei, resulting in oscillations of electron cloud, a dipole, Figure 6b and Figure 5 ($n = 1$ mode-1 electric lines of force). The dipole oscillation is most prominent, for small

spheres, with circumference of the order of wave length of EM radiation inside the metal ($2\pi R \sim \lambda_{\text{inside}}$, say, 10 microns). For still larger size of metal spheres electric Quadra-pole and higher modes are formed, which has half electron cloud oscillating parallel and remainder oscillates anti-parallel (Figure 5, mode-2 electric lines of force). From above derivations of previous sections, we found that the primary EM fields excite certain 'partial oscillations' in the spherical particle. These are not the natural modes of sphere for all are synchronous with the applied field. These partial oscillations and their associated fields, however, are Electric and Magnetic type for some reasons that were set forth with $a_n^{r,t}$ are the amplitudes of oscillations of magnetic type and $b_n^{r,t}$ are amplitudes of oscillations of electric type. Figure 5 gives the first four modes of these Mie solutions [6], for partial modes for Electric and Magnetic lines of forces.

The incident microwave radiation is linearly polarized, travelling in z with $\mathbf{E}$ vector towards x axis. At large distance from the spherical particle the radial component of the secondary field varies as $1/r^2$ while tangential components $\mathbf{E}_{r\theta}$ and $\mathbf{E}_{r\varphi}$ varies as $1/r$. In this radiation zone the field is transverse to the direction of propagation. These tangential components are perpendicular to each other and generally differ in phase. The secondary radiation from the spherical particle is elliptically polarized. There are two exceptional directions, note that when $\varphi = 0$, $\mathbf{E}_{r\varphi} = 0$ and when $\varphi = 90°$, $\mathbf{E}_{r\theta} = 0$. Meaning that when viewed along x- or the y- axis, the secondary radiation is linearly polarized. Inversely if the primary EM field is un-polarized, the secondary field is partially polarized depending on the direction of observation.

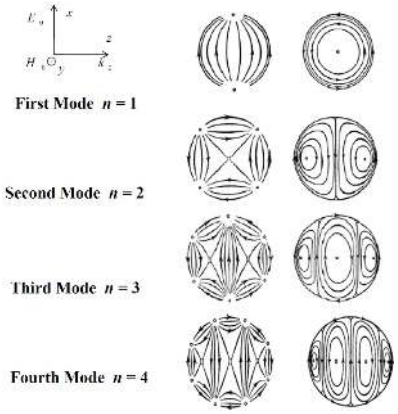

Figure 5. Electric and magnetic lines of forces of first four modes of partial oscillation on sphere.

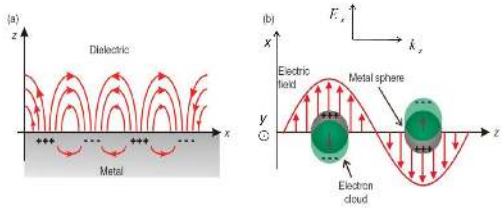

Surface effect depicted for EM radiation interacting with metal. The figure-a depicts plane surface interaction, and figure-b depicting the Surface effect is bounded by small spherical metal spheres, where the Electron cloud oscillates in synchronism with the oscillating E-field. The principal mode n=1 is depicted as dipole formation

Figure 6. Interaction of metal and EM radiation.

4. Absorption of Microwave Energy in Scattering via Spherical Particle and Expansion Coefficients

The resultant field at any point outside the sphere of Figure 4 is the 'total-radiation'; that is sum of incident field and reflected field.

$$\mathbf{E} = \mathbf{E}_i + \mathbf{E}_r, \qquad \mathbf{H} = \mathbf{H}_i + \mathbf{H}_r. \tag{32}$$

The radial component of the total complex energy flow vector is [4, 6]

$$\begin{aligned} \mathbf{S}_r^* &= \frac{1}{2}\mathbf{E}\times\overline{\mathbf{H}} = \frac{1}{2}(E_\theta \overline{H}_\varphi - E_\varphi \overline{H}_\theta) \\ &= \frac{1}{2}[(\mathbf{E}_i + \mathbf{E}_r)\times(\overline{\mathbf{H}}_i + \overline{\mathbf{H}}_r)] \\ &= \frac{1}{2}\mathbf{E}_i \times \overline{\mathbf{H}}_i + \frac{1}{2}\mathbf{E}_r \times \overline{\mathbf{H}}_r + \frac{1}{2}\mathbf{E}_i \times \overline{\mathbf{H}}_r + \frac{1}{2}\mathbf{E}_r \times \overline{\mathbf{H}}_i. \end{aligned} \tag{33}$$

After resolving we get three terms for energy flow as following:

$$\mathbf{S}_r^* = \frac{1}{2}(E_{i\theta}\overline{H}_{i\varphi} - E_{i\varphi}\overline{H}_{i\theta}) + \frac{1}{2}(E_{r\theta}\overline{H}_{r\varphi} - E_{r\varphi}\overline{H}_{r\theta}) + \frac{1}{2}(E_{i\theta}\overline{H}_{r\varphi} + E_{r\theta}\overline{H}_{i\theta} - E_{i\varphi}\overline{H}_{r\theta} - E_{r\varphi}\overline{H}_{i\theta}). \quad (34)$$

The real part of $\mathbf{S}_r^*$ integrated over a sphere of radius R concentric to the spherical particle which is diffracting the EM field (Figure 3), and is just outside the particle, is equal to net flow of energy across its surface. If the external medium, i.e., medium-2 is perfectly dielectric, having wave vector $k_2 = \omega\sqrt{\varepsilon_2\mu_2}$; and the spherical particle is assumed to be non-conducting; then the net flow across any surface enclosing the particle sphere, must be zero. If however, the energy is converted as heat within the sphere, the net flow is equal to the amount absorbed and is directed into the sphere. The total energy absorbed by sphere is [4, 6]

$$W_a = -\operatorname{Re}\int_0^{\pi}\int_0^{2\pi} S_r^* R^2 \sin\theta d\varphi d\theta. \quad (35)$$

The first term in expanded resolved expression (34) of $\mathbf{S}_r^*$ is the flow of energy in the incident EM field. When this is integrated over a closed surface, this gives zero as long as the medium is non conducting, i.e., $\sigma_2 = 0$. The second term (34) is outward flow of energy for the secondary scattered radiation from the diffracting sphere. This scattered energy is [4, 6]

$$W_s = \frac{1}{2}\operatorname{Re}\int_0^{\pi}\int_0^{2\pi}(E_{r\theta}\overline{H}_{r\varphi} - E_{r\varphi}\overline{H}_{r\theta})R^2 \sin\theta d\theta d\varphi. \quad (36)$$

The third term in the expression (34) of $\mathbf{S}_r^*$ must be equal to in magnitude to the sum of absorbed and scattered energies, meaning

$$W_t = W_a + W_s = \frac{1}{2}\operatorname{Re}\int_0^{\pi}\int_0^{2\pi}(E_{i\theta}\overline{H}_{r\varphi} + E_{r\theta}\overline{H}_{i\varphi} - E_{i\varphi}\overline{H}_{r\theta} - E_{r\varphi}\overline{H}_{i\theta})R^2 \sin\theta d\theta d\varphi. \quad (37)$$

W_t is therefore is the total energy derived from the primary EM field and is dissipated as heat and scattered radiation. To calculate W_s and W_t, we make $r \to \infty$ and use asymptotic values for $j_n(x)$ and $h_n^{(1)}(x)$, as indicated in previous sections; putting them in the expressions of field functions that is $\mathbf{E}_i$, $\mathbf{H}_i$ and $\mathbf{E}_r$, $\mathbf{H}_r$, then evaluating the integral above by help of following identities for Legendre polynomial [7]

$$\int_0^{\pi}\left(\frac{dP_n^1}{d\theta}\frac{dP_m^1}{d\theta}+\frac{1}{\sin^2\theta}P_n^1P_m^1\right)\sin\theta d\theta$$

$$=\begin{cases}0, & n\neq m,\\ \dfrac{2}{2n+1}\dfrac{(n+1)!}{(n-1)!}n(n+1), & n=m,\end{cases} \tag{38}$$

$$\int_0^{\pi}\left(\frac{P_m^1}{\sin\theta}\frac{dP_n^1}{d\theta}+\frac{P_n^1}{\sin\theta}\frac{dP_m^1}{d\theta}\right)\sin\theta d\theta=0. \tag{39}$$

The mean energy flow in z direction per unit area (m^2) is [4, 6]

$$\langle S_z\rangle=\frac{1}{2}E_0^2\sqrt{\frac{\varepsilon_2}{\mu_2}}. \tag{40}$$

For completion, we define the cross-sections of various scattering terms. The scattering cross section [4, 6] is defined as the ratio of the total scattered energy per second to the energy density of the incident EM field, that is, $Q_s = W_s / \langle S_z \rangle$. Thus the scattered energy and scattering cross section is

$$W_s=\pi\frac{E_0^2}{k_2^2}\sqrt{\frac{\varepsilon_2}{\mu_2}}\sum_{n=1}^{\infty}(2n+1)\left(\left|a_n^r\right|^2+\left|b_n^2\right|^2\right),$$

$$Q_s=\frac{2\pi}{k_2^2}\sum_{n=1}^{\infty}(2n+1)\left(\left|a_n^r\right|^2+\left|b_n^2\right|^2\right)\mathrm{m}^2. \tag{41}$$

The sum of absorbed and scattered energy and its cross section $(Q_t = W_t / \langle S_z \rangle)$, is

$$W_t = \pi \frac{E_0^2}{k_2^2} \sqrt{\frac{\varepsilon_2}{\mu_2}} \operatorname{Re} \sum_{n=1}^{\infty} (2n+1)(a_n^r + b_n^r),$$

$$Q_t = \frac{2\pi}{k_2^2} \operatorname{Re} \sum_{n=1}^{\infty} (2n+1)(a_n^r + b_n^r)\,\mathrm{m}^2. \tag{42}$$

If the conductivity or the inductive capacity $\varepsilon_1 / \varepsilon_2$, relative to the surrounding is large, that is, $|mx| >> 1$, then

$$Q_s \approx \frac{2\pi}{k_2^2} \sum_{n=1}^{\infty} (2n+1)(\sin^2 \gamma_n + \sin^2 \gamma_n'),$$

$$Q_t \approx \frac{2\pi}{k_2^2} \operatorname{Re} \sum_{n=1}^{\infty} i(2n+1)(e^{i\gamma_n} \sin \gamma_n + e^{i\gamma_n'} \sin \gamma_n'). \tag{43}$$

For non absorbing spherical particle, γ_n and γ_n' are real, and we get $Q_s = -Q_t$.

5. Approximations for Expansion Coefficients

5.1. The case when radius of spherical particle is larger than wavelength of EM field inside the particle $|x| = |k_1 R| >> 1$

The expansion coefficients are difficult to evaluate. Thus we can have limiting cases, the first one being $|x| = |k_1 R| >> 1$ meaning $R >> \lambda_1 / 2\pi$ radius of particle is several times the wave length of the EM wave inside the sphere. For this case, we get [7]

$$a_n^r \cong i^n e^{-ix} \frac{\mu_1 \sin a - \mu_2 m \cos a \tan b}{\mu_1 - i\mu_2 m \tan b},$$

$$b_n^r \cong -i^{n+1} e^{-ix} \frac{\mu_1 \cos a \tan b - \mu_2 m \sin a}{\mu_1 \tan b + i\mu_2 m}, \tag{44}$$

$$a = x - \frac{n+1}{2}\pi, \qquad b = mx - \frac{n+1}{2}\pi. \tag{45}$$

The expansion coefficients are oscillating functions $x = k_1 R$ and n, oscillating between zero and one. If for a_n^r, we replace n by $n+1$, then $a_{n+1}^r \cong b_n^r$, meaning

the amplitude of electric oscillations of order n has same amplitude of magnetic oscillations of next higher order.

5.2. The case when radius of spherical particle is smaller than wavelength of EM field inside the particle $|x| = |k_1 R| << 1$

The approximations [7] for spherical Bessel's and Henkel's functions are

$$j_n(x) = 2^n \frac{n!}{(2n+1)!} x^n \left(1 - \frac{n+1}{(2n+1)(2n+3)} x^2 + \ldots\right),$$

$$h_n^{(1)}(x) = \frac{i}{2^n} \frac{(2n)!}{n!} \frac{1}{x^{n+1}} + \ldots , \tag{46}$$

$$a_n^r \cong -i \frac{2^{2n} n!(n+1)!}{(2n)!(2n+1)!} \frac{x^{2n+1}}{\mu_1 n + \mu_2 (n+1)} A,$$

$$A = \left\{\mu_2 - \mu_1 - \frac{\mu_2[(n+1) + (n+3)m^2] - \mu_1[(n+3) + (n+1)m^2}{(2n+2)(2n+3)} x^2\right\}, \tag{47}$$

$$b_n^r \cong i \frac{2^{2n} n!(n+1)!}{(2n)!(2n+1)!} \frac{x^{2n+1}}{\mu_1 (n+1) + \mu_2 m^2 n} B,$$

$$B = \left\{\mu_1 - \mu_2 m^2 - \frac{\mu_1[(n+1) + (n+3)m^2] - \mu_2 m^2[(n+3) + (n+1)m^2}{(2n+2)(2n+3)} x^2\right\}. \tag{48}$$

For $|x| << 1$ further simplification gives

$$a_1^r \cong \frac{i}{3} \frac{x^3}{\mu_1 + 2\mu_2} \left\{\mu_1 - \mu_2 - \frac{1}{5}[\mu_1(2 + m^2) - \mu_2(1 + 2m^2)]x^2\right\}, \tag{49}$$

$$a_2^r \cong \frac{i}{15} \frac{\mu_1 - \mu_2}{2\mu_1 + 3\mu_2} x^5, \tag{50}$$

$$b_2^r \cong \frac{2i}{3} \frac{x^3}{2\mu_1 + \mu_2 m^2} \left\{\mu_1 - \mu_2 m^2 - \frac{1}{10}[\mu_1(1 + 2m^2) - \mu_2(2 + m^2)]x^2\right\}, \tag{51}$$

$$b_2^r \cong \frac{i}{15} \frac{\mu_1 - \mu_2 m^2}{3\mu_1 + 2\mu_2 m^2} x^5. \tag{52}$$

If $\mu_1 = \mu_2$, then further simplified expressions are

$$a_1^r \cong \frac{i}{45}(m^2-1)x^5, \qquad b_1^r \cong -\frac{2i}{3}\left(\frac{m^2-1}{m^2+2}x^3 - \frac{1}{10}\frac{m^4-1}{m^4+2}x^5\right),$$

$$b_2^r \cong -\frac{i}{15}\frac{m^2-1}{2m^2+3}x^5. \tag{53}$$

When the ratio of radius to wavelength is so small that x^5 can be neglected w.r.t. x^3, only first order electric oscillations need be taken into account that is b_1^r (and not a_n^r).

$$b_2^r \cong -\frac{2i}{3}\frac{m^2-1}{m^2+2}x^3 = -\frac{2i}{3}x^3\frac{\varepsilon_1-\varepsilon_2}{\varepsilon_1+2\varepsilon_2}. \tag{54}$$

5.3. The total power absorbed by small spherical metal particle

Equation (5) of $w(\mathbf{r})$ requires the knowledge of local amplitudes of the EM field, and thus is not very suitable for analytical investigation. The absorbed power by spherical particle is $W_a = W_t - W_s$. Using (41) and (42) as derived in previous sections, we have from Mie solution the analytical expression, we write power absorbed by a spherical particle irradiated by plane EM wave as

$$W = -\pi\frac{E_0^2}{k_2^2}\sqrt{\frac{\varepsilon_2}{\mu_2}}\sum_{n=1}^{\infty}(2n+1)[\,\mathrm{Re}(a_n^r + b_n^r) + |\,a_n\,|^2 + |\,b_n\,|^2. \tag{55}$$

When the centre of the particle is placed at $E_{\max}$ of standing wave (oven), then we have approximation (56), [8]

$$W_E = -\pi\frac{E_0^2}{k_2^2}\sqrt{\frac{\varepsilon_2}{\mu_2}}\sum_{n=1}^{\infty}(2n+1)(\,\mathrm{Re}[1+(-1)^n]^2 a_n^r + [1-(-1)^n]^2 b_n^r\} + [1+(-1)^n]^2|\,a_n^r\,|^2 + [1-(-1)^n]^2|\,b_n^r\,|^2. \tag{56}$$

When spherical particle placed in magnetic field maxima $H_{\max}$ of the standing wave (oven), we get approximation (57), [8]

$$W_H = -\pi\frac{E_0^2}{k_2^2}\sqrt{\frac{\varepsilon_2}{\mu_2}}\sum_{n=1}^{\infty}(2n+1)(\mathrm{Re}\{[1-(-1)^n]^2 a_n^r + [1+(-1)^n]^2 b_n^r\} + [1-(-1)^n]^2|\,a_n^r\,|^2 + [1+(-1)^n]^2|\,b_n^r\,|^2. \tag{57}$$

Although all the above expressions we are getting as infinite series in practice just a few terms is sufficient for small particles $x << 1$. The microwave power absorbed for various spherical material of different $\tan\delta$ is shown in Figure 5, where the placement of spherical particle is at $E_{\max}$ and $H_{\max}$ of standing wave inside oven cavity resonator.

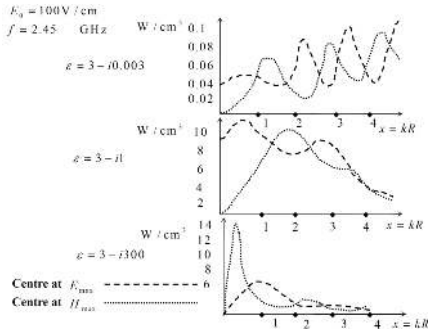

Figure 7. Power absorbed by spherical sample placed in Electric Maxima and Magnetic Maxima, with respect to size parameter $x = kR$.

From Figure 7; third plot, it is seen that heating in $H_{\max}$ position is better for samples with high electrical conductivity $\delta =\sim 90°$, with dimensions, not much smaller than skin depth. For sample with $\varepsilon = 3 - i300$, the skin depth is $l = 0.156\,\text{cm}$; with $kR = 1$ (in Figure 7) means $R = 1.9\,\text{cm}$, at 2.45 GHz microwave radiation. Figure 7 also shows that heating at electric field maximum position is better for spherical samples with low and moderate dielectric loss $(\tan\delta)$ and for very small samples (much smaller than skin depth). The skin depth for $\varepsilon = 3 - i0.003$ is $1556\,\text{cm}$, with $\tan\delta = 10\times10^{-4}$. For $\varepsilon = 3 - i1$, the skin depth is $6.8\,\text{cm}$ with $\tan\delta = 0.33$, for 2.45 GHz microwave radiation. When the spherical sample size is large, say for $x >> 1$ (larger than wavelength), heating equally effective in electric and magnetic maxima.

In earlier section, we stated that metal powder has thin coating of oxide insulator, and via EMA the effective property was also calculated. Figure 8 shows the highly conductive core of $\varepsilon_c = 12 - i10^4$, with presence of thin insulator of oxide $d = t/R$ has effective permittivity values much different from pure reflecting metal. The modification in loss tangent in presence of various thin mantle of insulating oxide shows the initial high loss tangent gets substantially reduced.

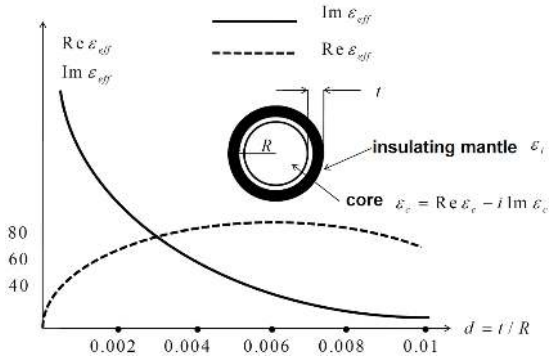

Figure 8. Effective dielectric permittivity in presence of mantle of insulator above spherical conducting shell with respect to mantle thickness.

This effect of reduction in loss tangent is advantageous in electric field absorption, for the metal powders, in other words aids the EM field absorption throughout the volume. Mapping of electric field in spherical sample is via aid of transmission (Mie) coefficients, (15)-(25). Use of these expressions gives the mapping of electric field inside spherical samples. Figure 9 plots the normalized square of electric field (E_t^2 / E_0^2) at $\theta = 0$ direction, gives idea of Electric energy released inside the sphere, for various values of ε_{eff} for a metal core $\varepsilon_c = 12 - i10^4$ covered by insulator $(\varepsilon_i = 4)$ of various specific thicknesses $(d = t/R)$.

Interesting inference can be drawn from Figure 9. When there is no insulation layer, the electric field penetrates and decays exponentially very fast within few fractions of centimeters into the sample. This is like skin deep penetration of Electric field into highly conductive sample. As the mantle insulator grows in thickness $(d = 0.004)$, the electric field penetrates more into the spherical sample and towards the centre. After some thickness $(d \sim 0.01)$, the electric field converges towards the centre of spherical sample, near the centre.

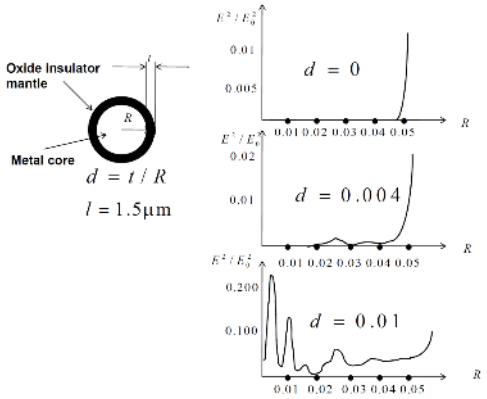

Figure 9. Square of normalized electric field mapping with respect to radius of spherical conducting shell for different insulating mantle thickness.

6. Observations

The square of electric field is measure of the value of power absorbed locally from the incident microwave radiation. With an increase in thickness of mantle of oxide layer around the conductive core metal, the electric field distribution of the absorbed power changes from a regular skin effect to a non uniform distribution that exhibits a spatial oscillatory structure of a specific scale associated with wave length inside the spherical particle (Figure 9). The field is having pronounced maximum towards the centre, which is specific to spherical shape and can be associated with converging of spherical electromagnetic wave. According to effective medium approximations the real part of effective permittivity is higher than imaginary part of effective permittivity for larger specific thickness of mantle; helps in making the electromagnetic field penetrate the sphere.

The above discussion was with one spherical particle in electromagnetic radiation. For a multi-particle system, we can scale the same theory by suitable multiplication; considering the multi-particle system does not interact with each other. The power absorbed by multi-particle system is thus

$$W_{\text{sample}} = NW_{\text{particle}}, \tag{58}$$

where W_{particle} comes from Mie solution of (55)-(57). The packing in sample, if we assume cubic lattice with spherical particles of radius R with separation between the particles as Δ, packed; then the expression of volume fraction in this cubic packing

is

$$\rho_f = \frac{\rho_c}{\left(1+\frac{\Delta}{2R}\right)^3}, \tag{59}$$

with, $\rho_c = \pi/6$ as percolation limit for the simple cubic lattice [23]. For separation distance Δ equal to 0.1 of diameter of the spherical particle, the ρ_f is 39% and for $\Delta = 0.2\times(2R)$ and $\Delta = 0.3\times(2R)$, the volume fraction of packing reduces to 30% and 24%, respectively. With this, we get number density N for use in (58) as [23], with V_{sample} and V_{particle} as volume of the sample and volume of the particle, respectively.

$$N = \frac{\rho_f V_{\text{sample}}}{V_{\text{particle}}}. \tag{60}$$

We can say for small sized spherical particles packed in the volume, when radius is smaller than wavelength the inter-particle interaction is small and above rule can be utilized for estimation of watt/volume of electromagnetic radiation absorbed by the sample several of spherical small metal powder particles packed in sample volume. For large sized spheres, the above estimation is invalid. In our bulk metal welding case Figure 1, we are packing the weld zone by the metal powder of approximately 40 micron diameter, and doing the process by microwave heating at 2.45 GHz. recently we did experiments on INCONEL-718 alloy joining by use of Nickel powder.

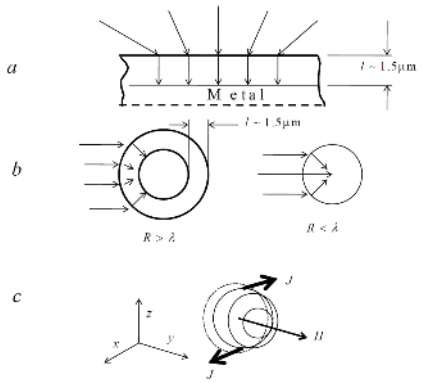

Figure 10. Summary of penetration of EM field into metal sphere and its convergence.

Figure 7 and Figure 9 give very interesting observation. From Figure 7, the curve number three, states that when we see at scales very similar to skin depth, the heating is due to $H_{\max}$. That is if we assume radius of metal-particle is very small $R < l$ smaller than skin depth, we would have EM absorption efficient if the particle is placed in $H_{\max}$. We assume that full penetration of magnetic field in this metal particle having radius lesser or compared to skin depth. The picture of this is depicted in Figure 10c. This magnetic field penetrates the particle induces a current which flows perpendicular to the external magnetic field. This current flows in the equatorial plane, the skin effect (via skin depth, l) imposes exponential dependence of current magnitude on the radius (r); that is,

$$J_1 \sim e^{\left[-\frac{(R-r)}{l}\right]}, \qquad J_2 \sim e^{\left[-\frac{(R+r)}{l}\right]}. \tag{61}$$

The currents J_1 and J_2 are induced diametrically opposite as shown in Figure 10c. Since we are talking of a spherical sample $R << l$, skin layers holding the currents as in (61) merge and penetrate, and we have resultant current superposition of the two currents, and when approximated, gives $J \cong 2|r|/l$, having maximum at $r = R$. This current gives Joule loss as proportional to J^2. Thus released power in small sphere due to Joule loss is proportional to R^2/l^2. This is induction heating of Figure 10c, via magnetic field for a spherical sample of size very small to skin depth. So we can infer that when a composite material contains conductive metal particles embedded in a low loss host material it absorbs microwave radiation due to magnetic polarization of particles [24]. The oscillating magnetic component induces electric currents (Figure 10c) in the particle, and depending on the size the currents may be stronger than that driven directly by Electric field (Figure 6b).

Most of the material processed by us for bulk metal welding is heterogeneous. For example metallic powder with oxide coating at all stages of densification remains two composite mixture of solid material in grains and voids between the grains. Composites formed as dielectric matrix of with metal particle inclusion (Figures 7, 8) are good absorbers of microwave radiation. Scale of micro-structural non uniformity is much less than electromagnetic wavelength inside the composite; and via average description the dielectric properties, the interaction of electric field is observed.

Whatever be the mode of absorption, either electric field or magnetic field of microwave radiation we have established that the volumetric penetration of energy

takes place and this is the most advantageous part in welding by use of microwave radiation. The temperature change of the volume is thus given by diffusion equation (62) with a source $w(\mathbf{r}) \sim \sigma_{\text{eff}}\mathbf{E}(\mathbf{r})$ right inside the sample volume. The source enters in scale of sub nano seconds as speed of propagation of microwave radiation into the volume, thus we call the inertia-less heat transfer. In (62) ρ, c_v κ are density, specific heat and thermal conductivity, respectively of the sample volume, and $T(\mathbf{r}, t)$ is the Temperature function of space-time.

$$\rho c_v \frac{\partial T(\mathbf{r}, t)}{\partial t} = \kappa \nabla^2 T(\mathbf{r}, t) + w(\mathbf{r}). \tag{62}$$

Therefore the difference between the conventional heating (say TIG welding) and microwave heating is volumetric heating, the heat is deposited directly inside the sample via $\mathbf{E}(\mathbf{r})$ or $\mathbf{H}(\mathbf{r})$. The thermal conduction expression (62) has volumetric heat source $w(\mathbf{r})$ in microwave heating case; whereas $w(\mathbf{r})$ is localized in near surface layer in conventional TIG welding. Figure 11 characterizes the joints done by microwave radiation.

The summary of microwave penetration to a highly conductive sample is explained in Figures 10a and 10b. The high refractive index makes the incident radiation to propagate normally to skin deep length inside the conductive sheet (Figure 10 a). The spherical conductive sample will refract all the EM radiation towards centre, but will propagate few microns inside the shell surface; however if the radius of spherical sample is small as few skin depths then radiations will be converging inside towards the centre; having maximum field near centre, (Figure 10b). If the radius is very small even smaller than skin depth then we get uniform field instead of spatially oscillating one as per Mie solution of transmittance and reflectance.

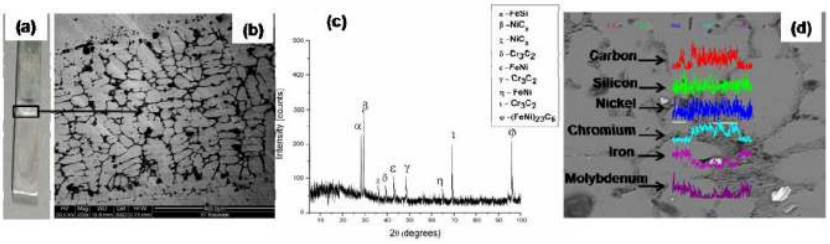

Figure 11. (a) Typical microwave processed SS-316 joints (b) Microstructure of joint zone (c) XRD spectra of the joint area (d) View of line mapping at the joint zone.

7. Conclusions

We have tried to explain the nature of heating that is volumetric inertia-less in nature what we observed in experiments of joining the bulk metals with use of metal powders via use of microwave radiation. The electrodynamics aspect of the Mie solutions in spherical coordinates gives insight of microwave energy profile of electromagnetic radiation inside spherical samples of metallic spheres. The discussion gives efficient heating in electric as well as magnetic field, and field penetration inside the sample of size comparable to few skin deep lengths. The penetration of the field is the cause of high heating rates as compared to conventional heating methods. Special studies in respect to field plot of multi layered spherical structure; experimental measurements of dielectric permittivity vis-à-vis temperature, mantle oxide layer for coated conductive metal powders, welding experiments with nano-sized powder, and with millimeter wave in this advanced welding method developed are planned as future advancements and studies.

8. Acknowledgements

This work is supported fully by Board of Research in Nuclear Science (BRNS), Department of Atomic Energy (DAE): the project is called MATERIAL JOINING & DRILLING WITH MICROWAVE. We acknowledge the encouragement received by Sri B. B. Biswas, Head Reactor Control Division, BARC; Sri G. P. Srivastava, Director E & I Group; Dr. R. K. Sinha, Director BARC and Chairman-AEC; Dr. S. Banerjee, Former-Chairman AEC; for inspiring us to do these experiments and Dr. A. L. Das, Director SAMEER to have helped us with equipments and his encouraging thoughts to take this experiment towards industrial usage in future. We acknowledge them all.

References

[1] A. K. Sharma, M. S. Srinath and Pradeep Kumar, Microwave joining of metallic materials, Indian Patent Appl. No. 1994/Del./2009.

[2] M. S. Srinath, A. K. Sharma and Pradeep Kumar, Investigation on micro-structural and mechanical properties of microwave processed dissimilar joints, J. Manufacturing 13(2) (2011), 141-146.

[3] Dheeraj Gupta and A. K. Sharma, Development and micro-structural characterization of microwave cladding on austenitic stailess steel, Surface & Coating Technology 205 (2011), 5147-5155.

[4] J. D. Jackson, Classical Electrodynamics, 3rd ed., Willey, New York, 1999.

[5] O. D. Kellogg, Foundation of Potential Theory, Springer-Verlag, Berlin, 1929.

[6] A. Stratton, Electromagnetic Theory, McGraw Hill, New York, London, 1941.

[7] M. Abramowitz and I. A. Stegun, eds., Handbook of Mathematical Functions, Dover, New York, 1965.

[8] R. Bhandari, Scattering coefficients for a multilayered sphere: analytic expressions and algorithms, Appl. Opt. 24(13) (1985), 1960-1967.

[9] C. F. Bohren and D. R. Huffman, Absorption and Scattering of Light by Small Particles, Wiley, Hoboken, NJ, 1983.

[10] W. Cai, Y. Zhao and L. Ma, Direct recursion of the ratio of Bessel functions with applications to Mie scattering calculations, J. Quant. Spectrosc. Radiat. Transfer 109(16) (2008), 2673-2678.

[11] L. A. Dombrovsky, Radiation Heat Transfer in Disperse Systems, Begell House, Redding, CT and New York, 1996.

[12] L. A. Dombrovsky and D. Baillis, Thermal Radiation in Disperse Systems: An Engineering Approach, Begell House, Redding, CT and New York, 2010.

[13] H. Du, Mie-scattering calculation, Appl. Opt. 43(9) (2004), 1951-1956.

[14] J. D. Felske, Z. Z. Chu and J. C. Ku, Mie scattering subroutines (DBMIE and MIEV0): a comparison of computational times, Appl. Opt. 22(15) (1983), 2240-2241.

[15] P. J. Flatau, SCATTERLIB: Light Scattering Codes Library, atol.uscd.edu/~pflatau/ scatlib/, 2000.

[16] J. P. Hosemann, Computation of angular functions π_n and τ_n occurring the Mie theory, Appl. Opt. 10(6) (1971), 1452-1453.

[17] G. W. Kattawar and G. N. Plass, Electromagnetic scattering from absorbing spheres, Appl. Opt. 6(8) (1967), 1377-1382.

[18] R. Li, X. Han, H. Jiang and K. F. Ren, Debye series for light scattering by a multilayered sphere, Appl. Opt. 45(6) (2006), 1260-1270.

[19] O. B. Toon and T. P. Ackerman, Algorithms for the calculation of scattering by stratified spheres, Appl. Opt. 20(20) (1981), 3657-3660.

[20] W. J. Wiscombe, Improved Mie scattering algorithms, Appl. Opt. 19(9) (1980), 1505-1509.

[21] T. Wriedt, Electromagnetic scattering programs, www.t-matrix.de, 2000.

[22] W. Yang, Improved recursive algorithm for light scattering by a multilayered sphere, Appl. Opt. 42(9) (2003), 1710-1720.

[23] D. J. Bergman and D. Stroud, Solid State Physics: Advances in Research and Application, H. Ehrenreich and D. Turnbull, eds., Academic Press, New York, Vol. 46, 1992, p. 147.

[24] L. D. Landau et al., Electrodynamics of Continuum Media, 2nd ed., Pergamon, New York, 1984.